



# **iJRASET**

International Journal For Research in  
Applied Science and Engineering Technology



---

# **INTERNATIONAL JOURNAL FOR RESEARCH**

IN APPLIED SCIENCE & ENGINEERING TECHNOLOGY

---

**Volume: 6**

**Issue: IX**

**Month of publication: September 2018**

**DOI:**

**[www.ijraset.com](http://www.ijraset.com)**

**Call:  08813907089**

**E-mail ID: [ijraset@gmail.com](mailto:ijraset@gmail.com)**

# Comparative Analysis of Solar Collector with V and W Shape Rib Roughened Absorber Plate for Air Heating Applications

Gauri Jadhav<sup>1</sup>, Dr. Vilas Pharande<sup>2</sup>

<sup>1, 2</sup>Department of Mechanical Engineering, Padmabhooshan Vasantdada Patil Institute Of Technology, Savitribai Phule Pune University, Maharashtra, India.

**Abstract:** Solar air heater is one of the best thermal collection equipment because it is easy to use and maintain. In general, for using smooth surface or plane plate of solar air heater, the energy saving in the form of thermal performance is quite low due to low convective heat transfer coefficient. It can be enhanced by employing passive methods in the form of artificial roughness on the absorber plate of solar air heaters. This paper presents results of a study of the performance of solar air heaters with W-shaped inline and staggered perforated fin as roughness on the air flow side of the absorber plate. Experimentation have been carried out by testing the under clear sky with available solar radiations intensity with variation in mass flow rate of air passing through collector for three different absorber plates. Collector efficiency has been calculated for plane absorber plate and compared with the absorber plate having inline and staggered W shape perforated rib roughened absorber plate. The results of the study are presented in the form of plots to show the effect of ambient, design and operating conditions collector efficiency.

**Keywords:** Solar air heater. Flat plate collector (FPC), Rib roughened surfaces, perforated fins

## I. INTRODUCTION

Energy is a decisive driving factor in today's world and plays foremost role in economic growth and industrial development. Population progression and its material needs increase the mandate of energy every year. On the other side, depletion of fossil fuel reduces the available resource and cause to environmental deprivation and it creates the consciousness towards renewable energy sources.

The maximum useful work of solar energy is needed to increase efficiency of the thermal collection apparatus. Solar air heater is one of the commonly used thermal collection equipment because it is easy to use and maintain. In general, for using smooth surface or plane plate of solar air heater, the energy saving in the form of thermal concert is quite low due to lower convective heat transfer. Solar air heater has low effectiveness because of low heat transfer coefficient between the air and absorber plate which leads to greater temperature of absorber surface due to which more thermal losses occurs. It was found that the major resistance to the convective heat transfer coefficient is due to the creation of the boundary layer on the heat conveying surface. Attempt has to be made to interrupt this layer by using artificially roughened planes. Artificial irregularity has been used to create the turbulence in the laminar sub layer.

Thus the artificial roughness can be used for the augmentation of heat transfer coefficient between the absorber plate and air, improving the thermal performance of solar air heater. Opposing to this by providing more disturbances across the layer will cause more pumping power essential which increase the friction which results in reduction of effective efficiency.

Solar collector efficiency can be enhanced by employing passive methods in the form of artificial irregularity on the absorber plate of solar air heaters. Numerous techniques have been developed for enhancing the heat transfer rate between the airflow and the absorber plate. In the solar air heater design, fin, baffle, rib, groove, wing and winglet are regularly introduced in order to increase the convective heat transfer rate leading to the compact heat exchanger and the increase in thermal performance. Another way of increasing the heat transfer rate is to employ ribs with perforations or disconnected ribs. The perforated ribs or blocks allow a part of the flow to pass through the punctures and hence the hot zone and form drag are decreased. Thus the perforated elements improve the heat transfer rate with lower pressure loss consequence.

This work aims to investigate the thermal performance of the solar flat plate collector with inline and staggered W shape perforated rib roughened absorber plat.

The performance of the collector has been predicted with variation in mass flow rate for three different absorber plates. Following are the research objectives for proposed work:

- 1) To study effect of artificially roughened absorber plate on the rate of heat transfer.
- 2) To find the instantaneous collector efficiency of flat plate solar collector at different mass flow rate of air.
- 3) To find the effect on instantaneous collector efficiency with Inline and staggered W-shaped perforated absorber plate solar collector.
- 4) To find the effect on temperature rise across the FPC with Inline and staggered W-shaped perforated absorber plate solar collector.

## II. LITERATURE REVIEW

Flat plate solar air heaters are commonly used in space heating and drying practices of agricultural products, clothing, herbal medicines etc. Because of minimal use of materials, this system inhabits an important place among solar thermal systems. There are various factors affecting the solar collector efficiency, e.g. collector geometry and dimensions, air velocity, type of absorber surface, glass cover plate etc. Enlarging the absorber area or fluid flow heat-transfer area increases heat transfer at the same time it increases the required power to pump the air flow through the collector. Various efforts have been made to increase the performance of flat plate solar collector for air heating systems and investigated by researchers. The use of an artificial roughness on the underside of the absorber plate is a superior technique to augment the rate of heat transfer to fluid flow in a solar air heater. The geometry of artificial irregularity is to be such that it should disrupt the laminar sub-layer for enhancing the heat transfer, and the core flow should not be unduly troubled to limit the increase in friction losses. In case of solar air heaters, rib type unevenness has been investigated typically. The ribs can be unbroken (full) or discrete (broken) depending on whether completes rib or the ribs in pieces are placed on the absorber plate. There are different shapes of the ribs like rectangular, circular, wedge, chamfered and orientation of the ribs can be as transverse, inclined and V-shaped. Many investigators analysed various roughness geometry and developed the correlations of the heat transfer coefficient and friction factor.

Varun, Saini R.P. and Singal S.K. [1] investigate the different techniques used by various researchers to enhance the thermal performance of solar air heater such as: artificial roughness, fins, ribs etc. Enhancement in thermal efficiency is obtained with different geometry of roughness. The use of artificial roughness on the surface of absorber surface is a promising technique to enhance the heat transfer between absorber plate and air flowing over it.

Prasad and Saini [2] investigate the relative roughness pitch and height effect on heat transfer and friction factor. They concluded with relations to calculate the average friction factor and Stanton number for artificial roughness of absorber surface by small diameter protuberance wire. It has been concluded that increase in the relative roughness height results in decrease of the rate of heat transfer enhancement.

Bhagoria et al [3] investigate to determine the outcome of relative roughness pitch, roughness height and wedge angle on the heat transfer and friction factor in a solar air heater roughened absorber plate having wedge shaped rib roughness. The presence of ribs increases Nusselt number up to 2.4 times while the friction factor increases up to 5.3 times as related to smooth duct in the range of limits investigated. An extreme enhancement in heat transfer was obtained at a wedge angle of about  $10^\circ$ .

Webb et al. [4] established heat transfer and friction correlations for turbulent flow in tubes having repeated rib roughness. The correlations determined 4 times higher efficiency with experimental figures taken with relative roughness height 0.01 to 0.04 and relative roughness pitch 10 to 40 and increases Prandtl number 0.71 to 37.6.

Gupta et al. [5] examined the effect of relative roughness height, angle of attack and Reynolds number on friction factor and heat transfer in rectangular duct having circular wire ribs on the absorber plate. The correlations were developed for Nusselt number and friction factor in terms of system and operating parameters. He concluded that the maximum heat transfer coefficient and friction factor were found at an angle of attack  $60^\circ$  and  $70^\circ$  in the range of parameters investigated. They also examined the thermo-hydraulic performance in relation of effective efficiency of solar air heater with rib roughened plate by using heat transfer and friction factor correlation developed by them.

Saini and Saini [6] investigate the effects of extended metal geometry as artificial roughness, and established the correlations for friction factor and Nusselt number. The maximum friction factor and Nusselt number occurred for relative short way length of mesh of 24 and 14 respectively. The maximum enhancement in Nusselt number and friction factor values were testified of the order of 4.5 and 6 times to the smooth absorber plate respectively.

Momin et al. Saini J.S. Solanki S.C. [7]. Heat transfer and friction in solar air heater duct with V-shaped rib roughness on absorber surface to study and increase more thermal efficiency. The investigation covered Reynolds number in the range of 3000–18,000, relative roughness height of 0.02–0.035 and angle of attack of flow of 30–90 for a fixed relative pitch of 10. For this V-shape ribs surface it was observed that the rate of increase of Nusselt number with an increase in Reynolds number is lower than the rate of

increase of friction factor. The extreme enhancement of Nusselt number and friction factor had been found as 2.30 and 2.83 times to smooth surface.

This work further extended by modifying the absorber surface with perforated W shaped ribs with inline and staggered arrangement. The variation in collector can also be evaluated with variation in mass flow rate of air passing through the collector.

### III. EXPERIMENTAL MATHEMATICAL DATA

Performance of solar heater should evaluate to know the effect of different modifications in absorber plate. For this purpose, the experimentally measured values are used and the results are discussed in terms of Nusselt number, friction factor, thermal efficiency. Method to estimate the above parameters are discussed below.

#### A. Heat Transfer Analysis

1) *Nusselt Number*: The heat transfer rate,  $Q_u$  to the air from absorber plate can be equated as,

$$Q_u = mC_p(T_{out} - T_{in}) \quad (1)$$

From Eqn. (1), experimental heat transfer coefficient can be determined and based on this experimental Nu (Nusselt number) can be calculated from following equation.

$$Nu = \frac{h_c D}{k} \quad (2)$$

2) *Friction factor*: Friction factor ( $f$ ) is the parameter used to calculate the frictional resistance of the fluid passing through the channel. It is related with the pressure drop across the channel.

$$f = \frac{\Delta p D}{2rLV^2} \quad (3)$$

#### B. Energy Efficiency

Energy efficiency measures the potential of solar air heater in energy conversion process. It is the ratio between useful heat gain to the incident solar radiation on collector area.

1) Heat input to the collector  $Q_{in}$

$$Q_{in} = \text{Aperture area} * \text{intensity of solar radiation}$$

$$\eta_I = \frac{Q_u}{Q_{in}} \quad (4)$$

#### C. Thermohydraulic Efficiency

Solar air heater is operated by using an electrical blower which converts the electrical energy into mechanical energy and forces the air through the heating system. The amount of energy required for the system is vary with the pressure drop due to expansion and contraction of heating system and frictional losses due to movement air absorber plate. These factors reduce the system efficiency and this pumping power is considered for evaluate the thermohydraulic efficiency of the system.

$$\eta_{THD} = \frac{Q_u - PP}{Q_{in}} \quad (5)$$

Where the pumping is calculated from

$$PP = \frac{FP}{\eta_{blower}} \quad (6)$$

$$FP = \frac{m\Delta p}{r} \quad (7)$$

### IV. DEVELOPMENT OF EXPERIMENTAL SET UP

Experimental system has been developed with Flat plate solar collector, flow regulating arrangement with orifice meter to measure the mass flow rate of air and the temperature sensors along with digital temperature indicator to measure the inlet and outlet temperature off the air and blower. A flat-plate collector consists of cover (the glazing) and a black coloured absorber plate. Solar radiation is absorbed by the absorber plate and transferred through an insulated metal box with a glass or plastic to air that circulates through the collector. The schematic diagram of the experimental set up is as shown in the Fig.1 the air taken from the atmosphere pressurises when it passes through the blower. The pressurised air then flows through the flow control valve where flow is regulated. Air then passes through the orifice meter, which is used to calculate the discharge. The air is fed to the solar collector where is absorbs the heat from the absorber plate which receives the heat from incident solar radiations. The heated air then taken out from the outlet of the collector. The temperature sensors (RTD) are mounted at inlet and outlet of the collector to measure the air inlet and outlet temperature.



**A. Flat Plate Collector**

The Flat Plate collector is used for air heating purpose. The air is supplied to the collector using blower. Physical parameters of the solar air heating systems are

Overall Size of the collector = Length \*Width \*Height =1000m\*800mm\*150mm

**B. Specifications of the Flat Plate collector:**

Reflecting material used = Aluminum

Dimensions of collector

Effective aperture area = 0.8 m<sup>2</sup>

Aperture width = 0.8 m

Length of collector: 1 m

Reflecting material used = Aluminum

Glass area = 0.8 m<sup>2</sup>

Collector glazing Window glass with 3 mm thickness

Bottom insulation 50 mm thickness of glass wool

The details of the three absorber plate are given below:

Absorber plate Width: 800 mm, length: 1000 mm

- 1) Plane plate
- 2) Absorber plate with Inline W shaped perforated ribs (Fig. 2)
- 3) Absorber plate with Staggered W shaped Perforated ribs (Fig.3)

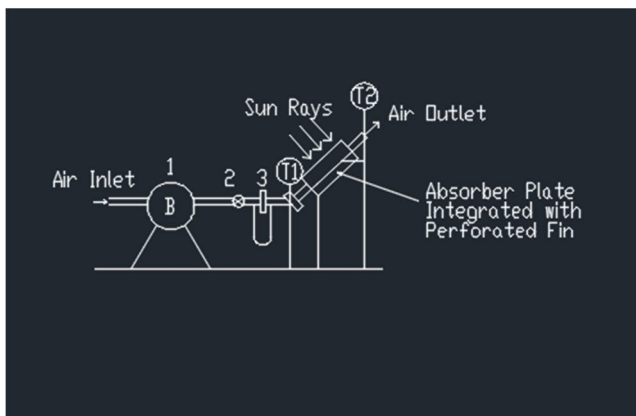


Fig.1: Schematic layout of experimental set up

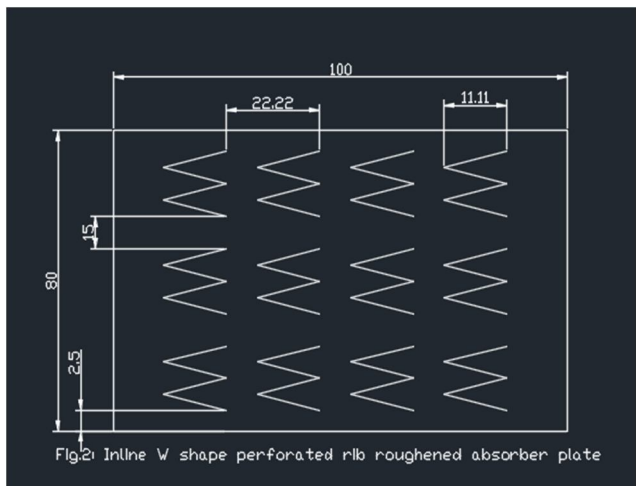


Fig.2: Inline W shape perforated rib roughened absorber plate

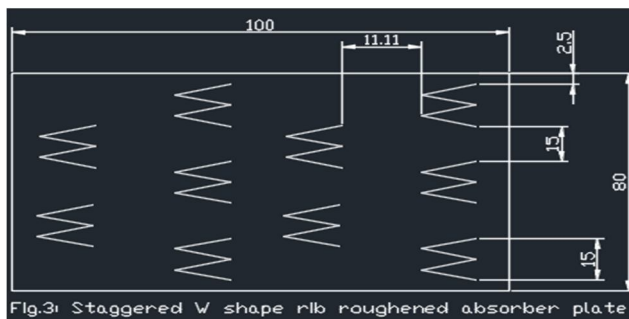


Fig.3: Staggered W shape rib roughened absorber plate

Specifications of Blower

Electric motor for blower – 0.5 HP, 1Ø, 230VAC, RPM = 2800

Specifications of Orifice meter with U-tube manometer:

The plate used in the orifice meter is having hole of 16 mm, and a manometer with range 200 -0 – 200 mm.

Specifications of Temperature indicator:

PT-100 type bare type and rod end type are used. Having range 0- 200 °C.

C. Test Methodology

A graphic view of single pass SAH is displayed in Figure1.placed at an inclination of 10° equal to latitude to receive possible utmost radiation.

Modified SAH is designed with turbulators (W shape turbulators) in the absorber plate to create turbulence effect. The modifications and number of turbulators are given in Figure 2 and in Figure 3.

Air blower (1hp) is connected with the flow control valve to provide appropriate quantity of air and flow rate is measured by adopting an orifice meter setup. Pressure drop across the test section is measured with the help of U-tube manometer. The temperature of the systems is measured in absorber plate (4 points), glass cover (2 points),inlet and outlet air by using K-type thermocouple. Thermocouples are linked with digital temperature indicator and selector switch arrangement. All the experiments were carried out from 9 am to 4 pm local time in the month of April 2018. Due to varying climatic condition, the experiments are operated at different days and discussion is made for average solar radiation and ambient temperature condition within the deviation of 10% for comparison purpose.

V. RESULTS AND DISCUSSION

Time(am/pm)	Solar Intensity Radiation (W/m <sup>2</sup> )		
	Flat Plate	Inline W shape Absorber Plate	Staggered W shape Absorber Plate
10:00	640	653	643
10:30	705	727	711
11:00	780	813	793
11:30	860	873	853
12:00	920	950	931
12:30	935	967	945
01:00	955	990	970
01:30	950	970	945
02:00	920	920	910
02:30	850	852	840
03:00	765	772	760
03:30	655	688	670
04:00	555	568	550
04:30	475	502	480
05:00	440	465	455

Table 1: Observation table for solar intensity radiations (W/m<sup>2</sup>)

It is assumed that amount of energy incident on the collector should be constant for all mass flow rates and for all the absorber plates at a given time. Variation in the intensity of solar radiation is recorded during the testing with respect to time and Fig.4 shows the variation intensity of solar radiation with time for mass flow rate of 0.01726 kg/sec for three absorber plates. It indicates that the variation in intensity of solar radiation with time for all plates for given mass flow rate is same, which indicates variation in intensity of solar radiation is same and same amount of energy is supplied to the all the absorber plates at a given time.

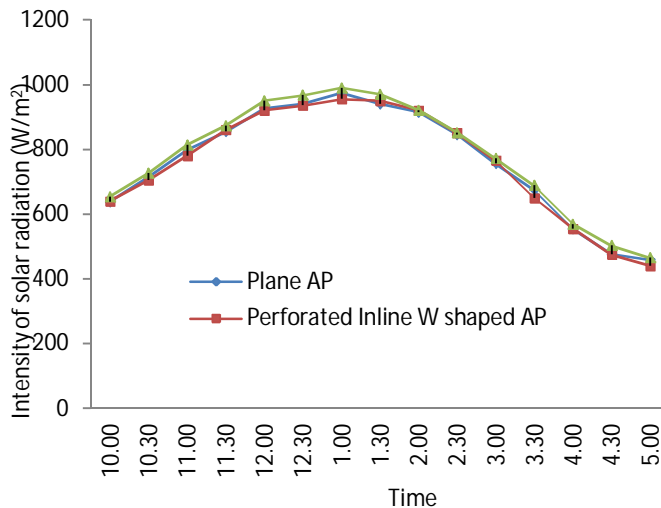


Fig.4 Variation of Intensity of Solar radiation with time at mass flow rate 0.01726 kg/sec

Fig. 4 shows the variation in intensity of solar radiation with time for mass flow rate of 0.01726 kg/sec for three absorber plates. It indicates that the variation in intensity of solar radiation with time for all plates for given mass flow rate is same, which indicates variation in intensity of solar radiation is same and same amount of energy is supplied to the all the absorber plates at a given time for all mass flow rates of air.

Fig. 5 to 8 shows the variation in the thermal efficiency of the FPC with plane absorber plate ,inline W-shaped perforated absorber plate and staggered W-shaped perforated absorber plate for 0.01726kg/sec mass flow rate of the air throughout the day from 10am to 5 pm. Below graphs shows that the instantaneous flat plate collector efficiency for staggered W shaped perforated absorber plate collector is higher by 13-25 % compared with plane absorber plate collector & 8-16 % higher compared with inline W-shaped perforated absorber plate.

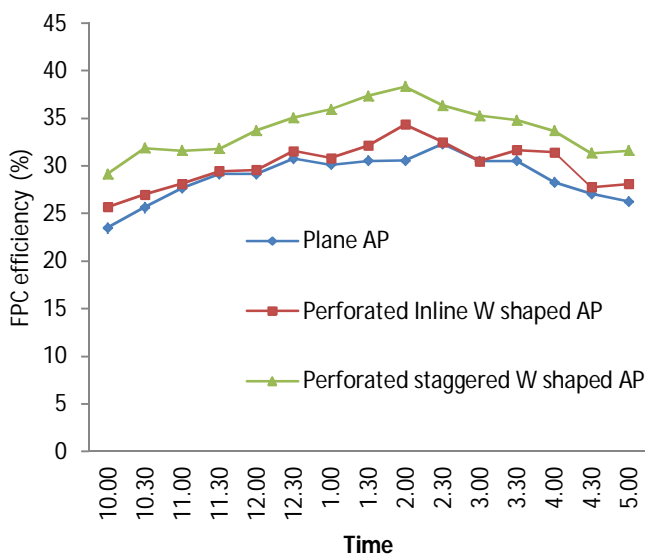


Fig.5 Variation of FPC efficiency with time at mass flow rate 0.01726 kg/sec

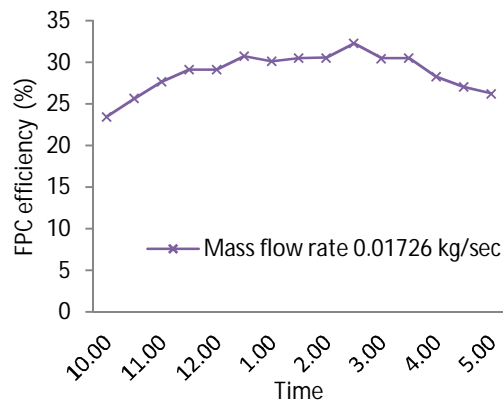


Fig.6 Variation of FPC efficiency with time for plane Absorber plate

Fig.6 shows the variation in the thermal efficiency of the FPC with plane absorber plate for 0.01726kg/sec mass flow rate of the air throughout the day from 10am to 5 pm. The maximum thermal efficiency obtained during experimentation is about 30-31% at around 2.00pm to 2.30pm for the maximum mass flow rate of 0.01726kg/sec.

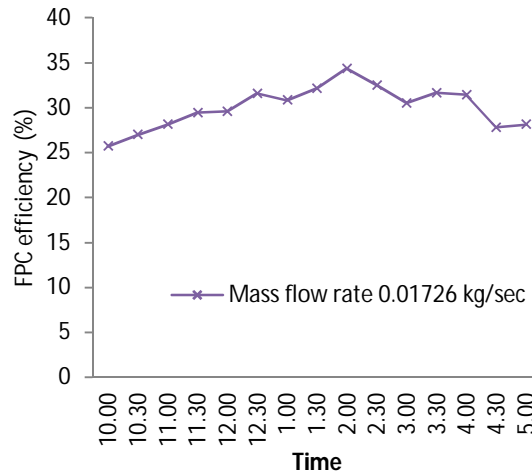


Fig.7 Variation of FPC efficiency with time for Perforated Inline W shaped fin absorber plate.

Fig.7 shows the variation in the thermal efficiency of the FPC with inline W shaped perforated absorber plate for 0.01726kg/sec mass flow rate of the air throughout the day from 10am to 5 pm. The maximum thermal efficiency obtained during experimentation is about 34-35% at around 2.00pm to 2.30pm for the maximum mass flow rate of 0.01726kg/sec.

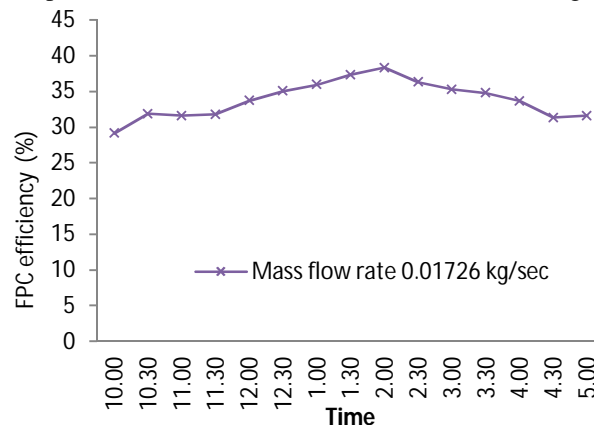


Fig.8 Variation of FPC efficiency with time for Perforated staggered W shaped fin absorber plate.



Fig.8 shows the variation in the thermal efficiency of the FPC with staggered W shaped perforated fin absorber plate for 0.01726kg/sec mass flow rate of the air throughout the day from 10am to 5 pm. The maximum thermal efficiency obtained during experimentation is about 37-38 % at around 2.00pm to 2.30pm for the maximum mass flow rate of 0.01726kg/sec.

Time(am/pm)	Temperature Rise		
	Flat Plate	Inclined W shape plate	Staggered W shape plate
10:00	6.9	7.7	8.6
10:30	8.3	9	10.4
11:00	9.9	10.5	11.5
11:30	11.5	11.8	12.4
12:00	12.3	12.9	14.4
12:30	13.2	14	15.2
01:00	13.2	14	16
01:30	13.3	14.3	16.2
02:00	12.9	14.5	16
02:30	12.6	12.7	14
03:00	10.7	10.8	12.3
03:30	9.1	10	10.7
04:00	7.2	8.2	8.5
04:30	5.9	6.4	6.9
05:00	5.3	6	6.6

Table2: Observation table for temperature rise

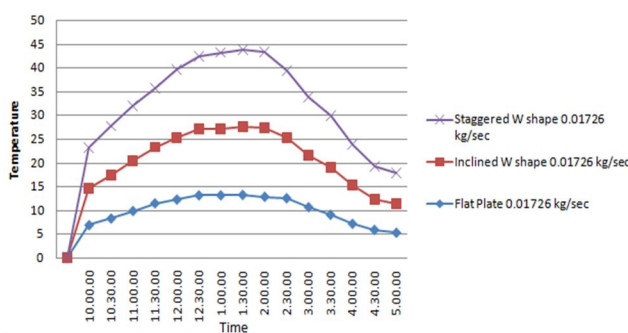


Fig.9 Variation of Temperature rise with time for Flat/Inline W shape/ Staggered W shape Absorber plate

The maximum temperature rise across the FPC with Staggered W shape absorber plate obtained during experimentation is about 15-16°C at around 2.00pm to 2.30pm for the maximum mass flow rate of 0.01726kg/sec.

## VI. CFD ANALYSIS

### A. Description Of Computational Model

Solar air heater duct having W-shaped perforated ribs has been considered for CFD investigation (Fig.6.1). W-shaped ribs having perforation were attached on the upperside of the plate. Thickness of ribs was taken 3 mm because small thickness ribs was more advantageous.

The investigation was done using software ANSYS CFD 16.0. ANSYS Design Modeler was used for preparing the 3-D fluid domain for analysis. Initially a coarse mesh was used to resolve the flow. The steady flow analysis was done using governing equations of energy, momentum and continuity. The solver used was segregated with finite volume based algorithm and second order upwind scheme was chosen for momentum, continuity and energy equations. For discretization of governing equations, SIMPLE algorithm was chosen. A constant heat flux condition of 1000 W/m<sup>2</sup> was applied on ribbed surface, while for other walls

adiabatic boundary condition was applied. All the other walls are considered to be completely insulated with zero heat flux. No slip condition is applied to all the ‘walls’. A uniform air velocity is introduced at the inlet while a pressure outlet condition is applied at the exit. At the exit, a pressure outlet boundary condition is specified with a fixed pressure of  $1.013 \times 10^5$  Pa. The convergence limit of  $10^{-4}$  for residual of continuity equation,  $10^{-4}$  for the residuals of velocity components and  $10^{-8}$  for residuals of energy was taken. After obtaining initial results, the mesh was made finer at specific locations to obtain the results.

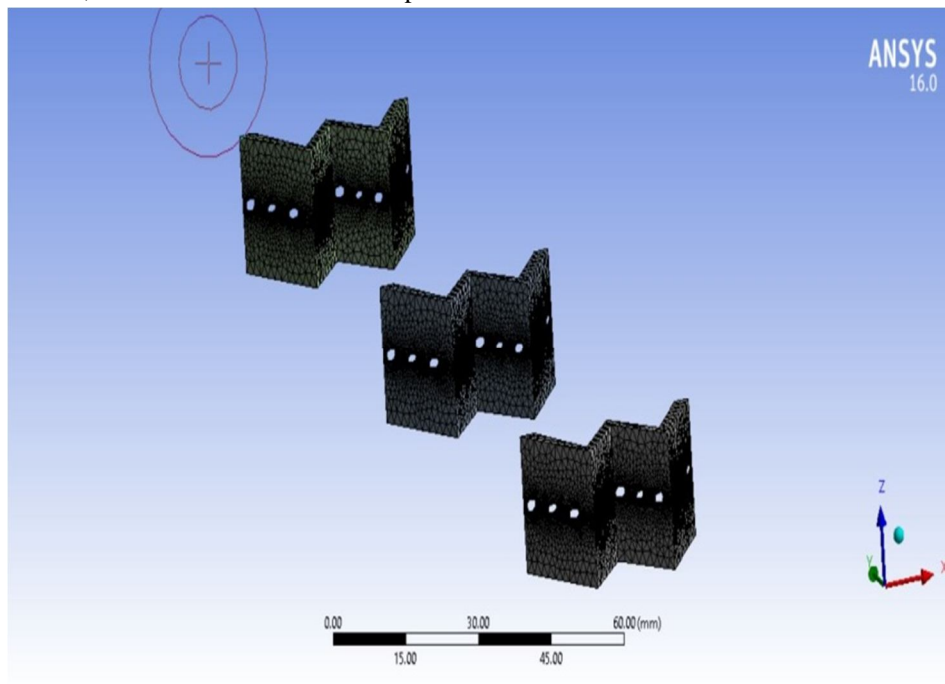


Fig.6.1 Meshing of W shaped ribs

Properties	Air	Absorber plate and W-Shaped ribs(aluminum)
Density, ' $\rho$ ' (kgm <sup>-3</sup> )	1.225	2719
Specific heat, ' $C_p$ ' (Jkg <sup>-1</sup> K <sup>-1</sup> )	1005	871
Viscosity, ' $\mu$ ' (Nsm <sup>-2</sup> )	1.84e-05	-
Thermal conductivity, ' $k$ ' (Wm <sup>-1</sup> K <sup>-1</sup> )	0.0242	202.4

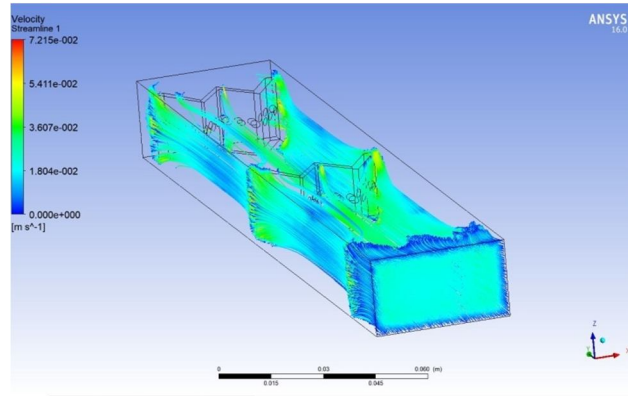


Fig. 6.2 Contour of stream function for the W shaped ribs

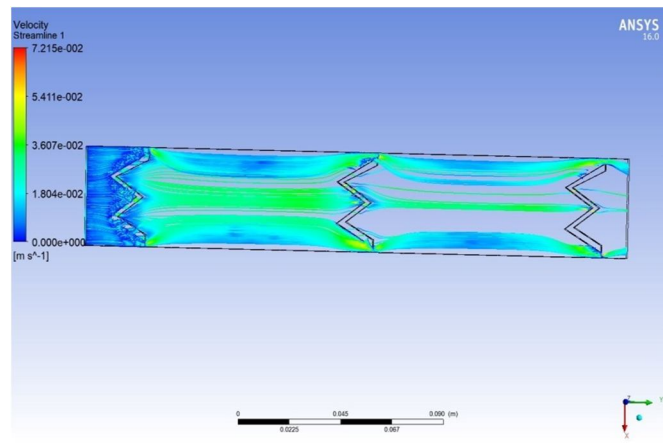


Fig. 6.3 Contour of stream function for W shaped ribs

Fig.6.2 and 6.3 shows the contour of stream function for w shaped ribs inserted in a solar heater duct. An observation of the stream function reveals that vortex formation near the ribs surface provides rolling action to the flow and hence reduces the friction. The heat transfer rate is maximum near the ends of the ribs and velocity is flowing in increasing rate. It also shows the velocity variation on the plate from inlet to outlet. On inlet section the velocity is almost zero because at absorber surface, air is in contact and boundary layer formation start. In test section where artificial roughness is provided the boundary layer formation is disturbed and hence velocity increases with respect to at the initial contact point. This disturbance in the boundary layer increases the heat transfer rate.

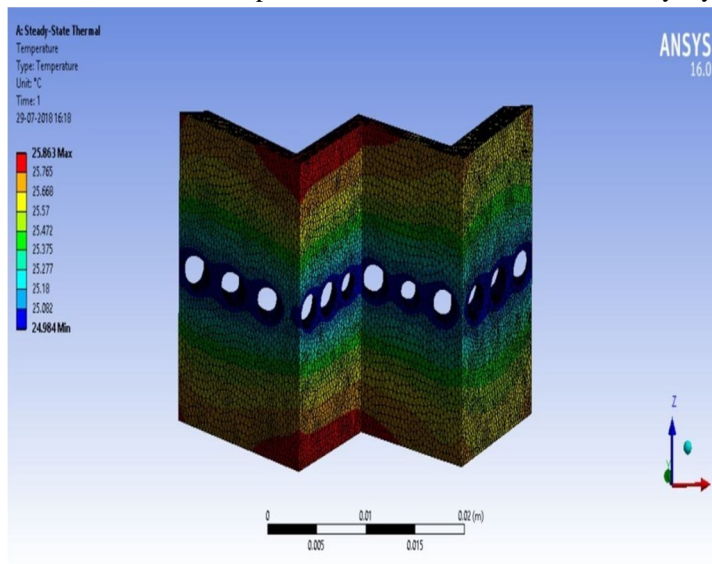


Fig. 6.4 Contour of temperature variation on W shape ribs

Fig. 6.4 shows the temperature Contour for the W shape of ribs inserted in a solar air heater duct. The patterns of temperature contour at regions up and down side of the rib illustrate the overall temperature field and the degree of heat transfer. CFD predicts temperature contour pattern better at the regions up and down side of the rib.

*B. Analysis of V shaped ribs*

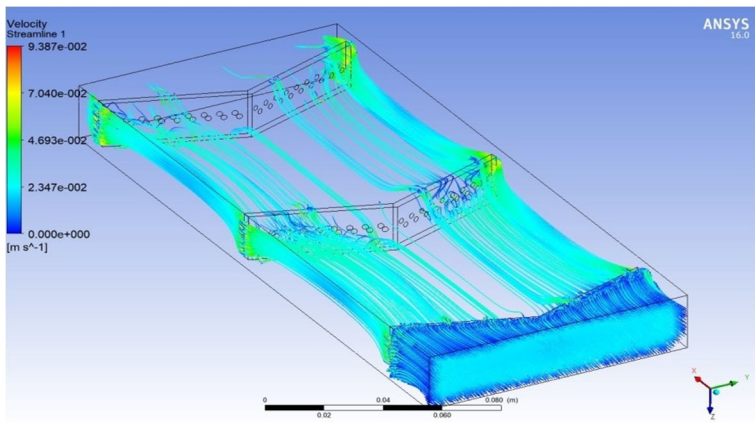


Fig.6.5 Contour of stream function for V shaped ribs

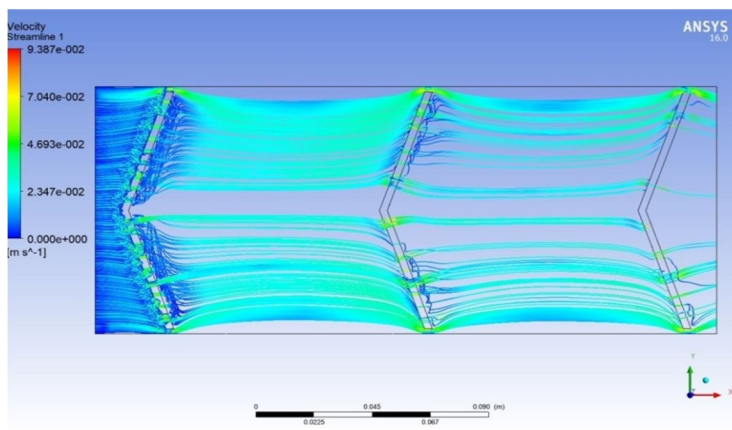


Fig.6.6 Contour of stream function for V shaped ribs

Fig. 6.5 and 6.6 shows the contour of stream function for the V shape of ribs inserted in a solar air heater duct. An observation of stream function contours reveals that vortex formation at top of the rib surface provides rolling action to the flow and hence reduces the friction. In this pattern , the divided secondary flow directed towards the side walls which allows higher heat extraction rates.

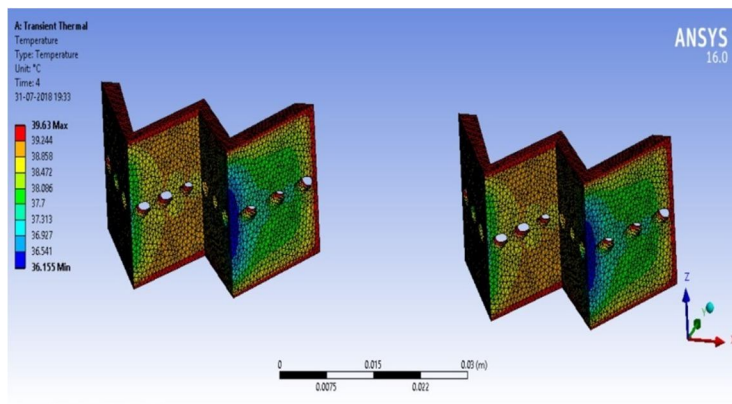


Fig 6.7 Contour of temperature of W shape ribs

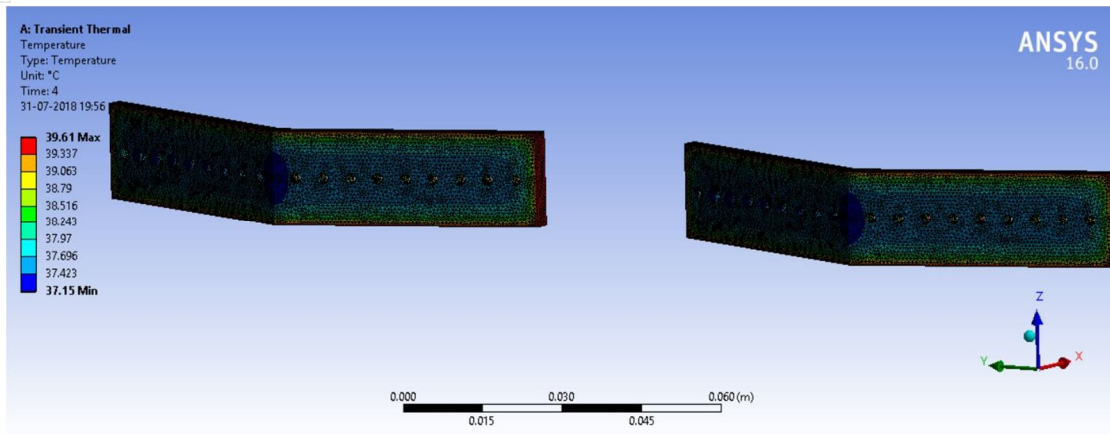


Fig.6.8 Contour of temperature of V shape ribs

Fig. 6.7 and 6.8 shows the contour of temperature for the W and V shape of ribs inserted in a solar air heater duct. An observation of temperature contours reveals that the temperature is varying all over the ribs, the maximum temperature attains near all the edges of the rib and perforations of the W shape rib. For V shape ribs the maximum temperature is obtained near the vortex side of the rib. The above contour shows the overall range of temperature on the surface of the rib for staggered W shape absorber plate having mass flow rate of 0.01484 m/s.

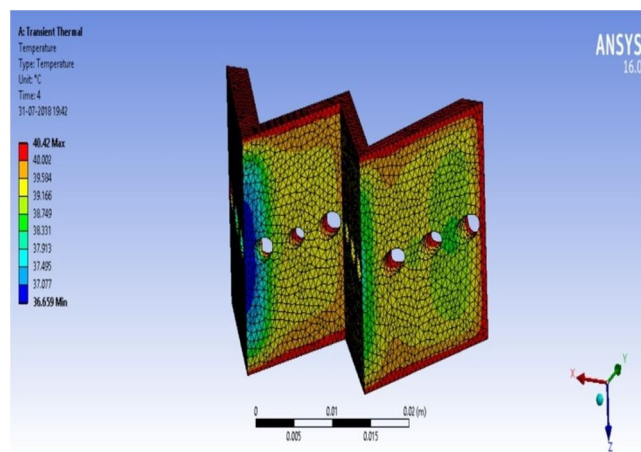


Fig 6.9 Contour of temperature of W shape ribs

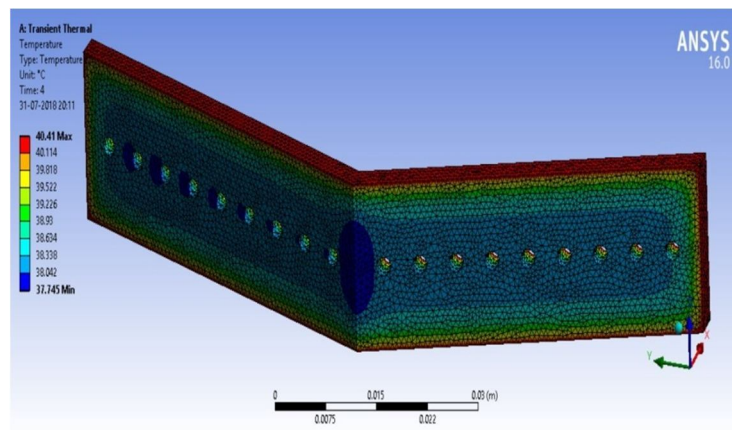


Fig. 6.10 Contour of temperature of V shape ribs

Fig. 6.9 and 6.10 shows the contour of temperature for the W and V shape of ribs inserted in a solar air heater duct. An observation of temperature contours reveals that the temperature is varying all over the ribs, the maximum temperature attains near all the edges of the rib and perforations of the W shape rib. For V shape ribs the maximum temperature is obtained near the vortex side of the rib.



The above contour shows the overall range of temperature on the surface of the rib for staggered W shape absorber plate having mass flow rate of 0.01569 m/s.

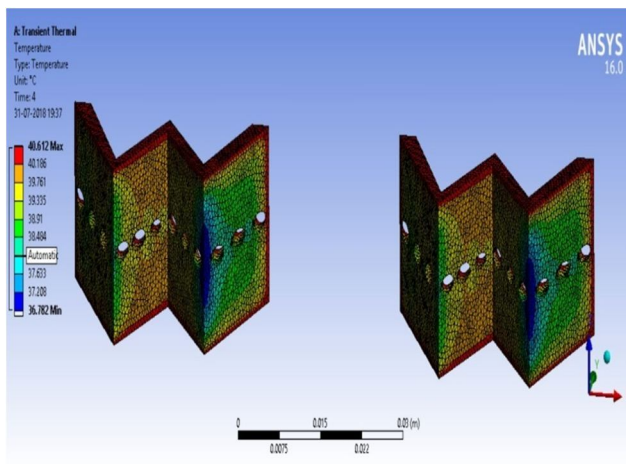


Fig. 6.11 Contour of temperature of W shape ribs

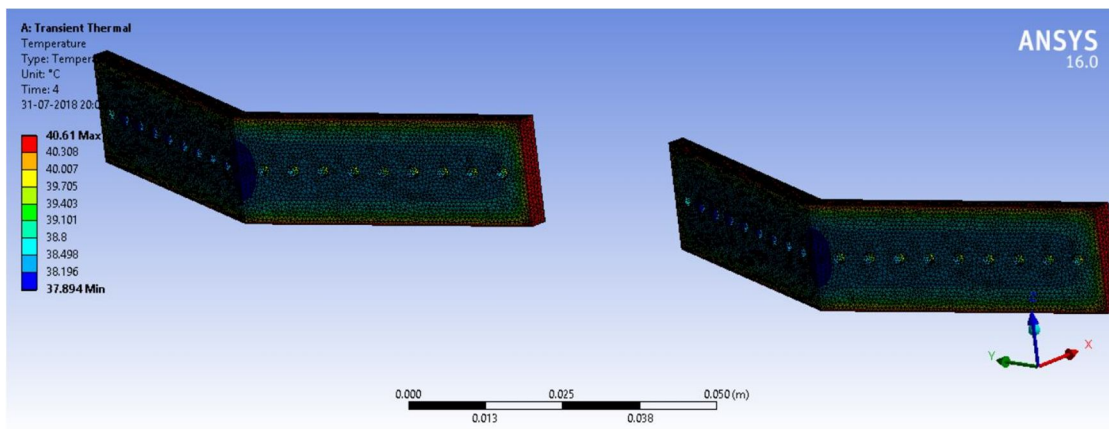


Fig. 6.12 Contour of temperature of V shape ribs

Fig. 6.11 and 6.12 shows the contour of temperature for the W and V shape of ribs inserted in a solar air heater duct. An observation of temperature contours reveals that the temperature is varying all over the ribs, the maximum temperature attains near all the edges of the rib and perforations of the W shape rib. For V shape ribs the maximum temperature is obtained near the vortex side of the rib. The above contour shows the overall range of temperature on the surface of the rib for staggered W shape absorber plate having mass flow rate of 0.01649 m/s.

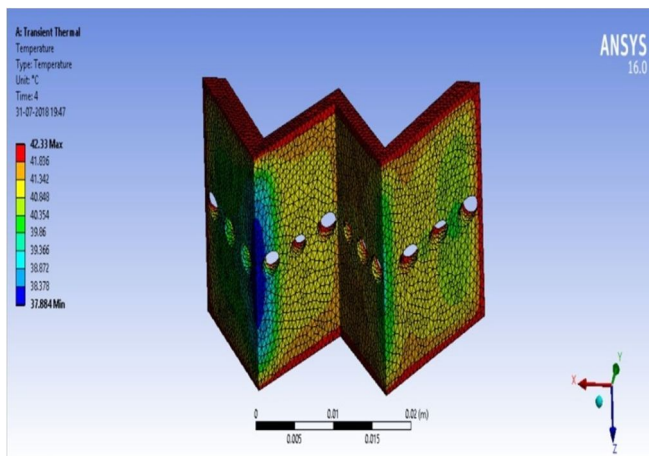


Fig. 6.13 Contour of temperature of W shape ribs

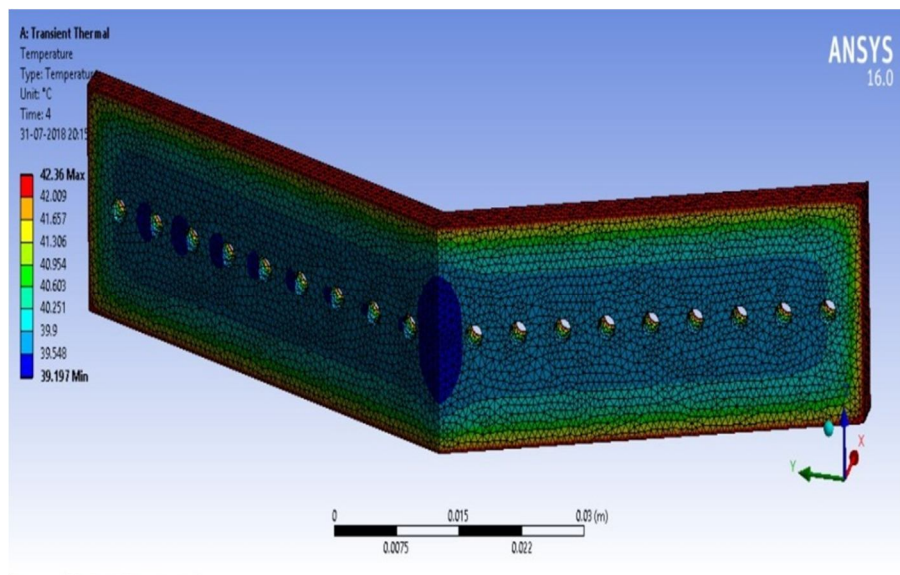


Fig. 6.14 Contour of temperature of V shape ribs

Fig. 6.13 and 6.14 shows the contour of temperature for the W and V shape of ribs inserted in a solar air heater duct. An observation of temperature contours reveals that the temperature is varying all over the ribs, the maximum temperature attains near all the edges of the rib and perforations of the W shape rib. For V shape ribs the maximum temperature is obtained near the vortex side of the rib. The above contour shows the overall range of temperature on the surface of the rib for staggered W shape absorber plate having mass flow rate of 0.01726 m/s.

## VII. CONCLUSION

In this study experimental performance evaluation has been carried to investigate the variation in instantaneous collector efficiency for inline and staggered W shape perforated rib roughened absorber plate solar collector and results are compared with that of plane plate absorber plate collector. The effect of variation in mass flow rate of the air on instantaneous collector efficiency has also been evaluated.

The following conclusions were drawn from this study.

Solar collector with artificially roughened absorber plate enhances the rate of heat transfer from absorber plate to air and thus increases the instantaneous collector efficiency of the solar collector. Thus results obtained from this study are in line with the findings of previous researcher.

- 1) The instantaneous collector efficiency of flat plate solar collector increases with increase in mass flow rate of air.
- 2) Enhancement obtained in instantaneous collector efficiency with staggered W-shaped perforated absorber plate solar collector ranges from 8-12 % as compared with inline W-shaped perforated absorber rib roughened absorber plate solar collector.
- 3) Enhancement obtained in instantaneous collector efficiency with staggered W-shaped perforated absorber plate solar collector ranges from 10-13 % as compared with plain absorber plate solar collector.
- 4) Temperature rise across the FPC is more 2-3 °C & 4-5 °C in case of staggered W-shaped perforated absorber plate solar collector as compared to two others that is plane absorber plate and inline W-shaped perforated absorber plate respectively.
- 5) The maximum temperature rise across the FPC in case of staggered W shaped perforated fin absorber plate is 8-12°C for the maximum mass flow rate of 0.01726 kg/sec.
- 6) In recent years CFD has been applied in the design of solar air heater. The studies reported that the quality of the solutions obtained from CFD simulations are largely within the acceptable range proving that CFD is an effective tool for predicting the behavior and performance of a solar air heater.
- 7) An attempt has been made to carry out CFD based analysis using ANSYS 16 to fluid flow and heat transfer characteristics of solar air heater having roughened duct provided with artificial roughness. Combined effect of turbulence and reattachment of fluid which was considered to be responsible in the increase of heat transfer rate.
- 8) The CFD analysis of W and V shape ribs reveals that maximum temperature has been found on the rib surface is between 39.6 – 42.3° for different mass flow rates on staggered W shape roughened absorber plate.

## REFERENCES

- [1] Varun, R.P. Saini, S.K. Singal. A review on roughness geometry used in solar air heaters. *Solar Energy*.2007; 81: 1340–1350. (2007)
- [2] Prasad B.N, Saini J. S. Effect of artificial roughness on heat transfer and friction factor in a solar air heater. *Solar Energy*. 1988;41(6): 555–560.(1988)
- [3] Bhagoria J. L, Saini J. S, Solanki SC. Heat transfer coefficient and friction factor correlations for rectangular solar air heater duct having transverse wedge shaped rib roughness on the absorber plate. *Renew Energy*. 2002; 25: 341–69(2002)
- [4] Webb RL, Eckert ERG. Heat transfer and friction in tubes with repeated-rib roughness. *Int J Heat Mass Transfer*1971;14:601–17.(1971)
- [5] Han JC, Zhang YM. High performance heat transfers ducts with parallel broken and V- shaped broken ribs. *Int J Heat Mass Transfer* 1992;35(2):513–23.(1992)
- [6] Gupta D, Solanki SC, Saini JS. Thermo-hydraulic performance of solar air heaters with roughened absorber plates. *Solar Energy* 1997;61:33–42.(1997)
- [7] Momin AME, Saini JS, Solanki SC. Heat transfer and friction in solar air heater duct with v- shaped rib roughness on absorber plate. *Int J Heat Mass Transfer*.2002;45:3383–96(2002)
- [8] Saini RP, Saini JS. Heat transfer and friction factor correlations for artificially roughened ducts with expanded metal mesh as roughened element. *Heat Mass Transfer*. 1997; 40: 973–86.(1997)
- [9] Verma SK, Prasad BN. Investigation for the optimal thermohydraulic performance of artificially roughened solar air heaters. *Renew Energy*. 2000; 20:19–36.(2000)
- [10] Saini SK, Saini RP. Development of correlations for Nusselt number and friction factor for solar air heater with roughened duct having arc-shaped wire as artificial roughness. *Solar Energy*. 2008; 82: 1118–30.(2008)
- [11] Karwa RK. Experimental studies of augmented heat transfer and friction in asymmetrically heated rectangular ducts with ribs on heated wall in transverse, inclined, v-continuous and v- discrete pattern. *Int Commun Heat Mass Transfer* 2003; 30: 241–50(2003)





10.22214/IJRASET



45.98



IMPACT FACTOR:  
7.129



IMPACT FACTOR:  
7.429



# INTERNATIONAL JOURNAL FOR RESEARCH

IN APPLIED SCIENCE & ENGINEERING TECHNOLOGY

Call : 08813907089  (24\*7 Support on Whatsapp)